Two developmentally distinct populations of neural crest cells contribute to the zebrafish heart

Ann M. Cavanaugh, **Jie Huang**, and **Jau-Nian Chen**[*]

Department of Molecular, Cell and Developmental Biology, University of California, Los Angeles, CA 90095, USA

Abstract

Cardiac neural crest cells are essential for outflow tract remodeling in animals with divided systemic and pulmonary circulatory systems, but their contributions to cardiac development in animals with a single-loop circulatory system are less clear. Here we genetically labeled neural crest cells and examined their contribution to the developing zebrafish heart. We identified two populations of neural crest cells that contribute to distinct compartments of zebrafish cardiovascular system at different developmental stages. A stream of neural crest cells migrating through pharyngeal arches 1 and 2 integrates into the myocardium of the primitive heart tube between 24 and 30 hours post fertilization and gives rise to cardiomyocytes. A second wave of neural crest cells migrating along aortic arch 6 envelops the endothelium of the ventral aorta and invades the bulbus arteriosus after three days of development. Interestingly, while inhibition of FGF signaling has no effect on the integration of neural crest cells to the primitive heart tube, it prevents these cells from contributing to the outflow tract, demonstrating disparate responses of neural crest cells to FGF signaling. Furthermore, neural crest ablation in zebrafish leads to multiple cardiac defects, including reduced heart rate, defective myocardial maturation and a failure to recruit progenitor cells from the second heart field. These findings add to our understanding of the contribution of neural crest cells to the developing heart and provide insights into the requirement for these cells in cardiac maturation.

Introduction

Neural crest (NC) cells are a population of ectodermally derived cells specified in the dorsal-most region of the neural tube. These cells migrate throughout the developing embryo to give rise to a wide variety of cell types, including smooth muscle, melanocytes, neurons, thymus and elements of the craniofacial skeleton (Le Douarin and Kalcheim, 1999; Hutson and Kirby, 2003). A subset of NC cells termed Cardiac Neural Crest (CNC) cells contributes to the heart. In chick and mouse, these cells originate between the otic vesicle and the third somite, migrate along a dorsolateral path and enter pharyngeal arches 3, 4, and 6 where they envelop the endothelium of aortic arch arteries and give rise to the smooth muscle layer of

[*]Correspondence to: chenjn@mcdb.ucla.edu.

the great vessels (Kirby et al., 1983; Jiang et al., 2000). Some CNC cells continue to migrate into the cardiac outflow tract (OFT) cushion to divide the common arterial OFT into the aorta and pulmonary trunks (Kirby et al., 1983; Jiang et al., 2000). Consistent with the contribution of these cells, mechanical ablation or genetic disruption of CNC development leads to ventricular septal defects, double outlet right ventricle, and persistent truncus arteriosus (Besson et al., 1986; Conway et al., 1997).

As CNC cells migrate through the pharynx, they interact extensively with neighboring tissues via a wide range of signaling molecules. FGF8 is one such signaling molecule that supports the survival and migration of CNC cells (Abu-Issa et al., 2002; Frank et al., 2002). FGF8 is expressed in multiple tissues in the pharyngeal apparatus. While knocking out FGF signaling in CNC cells does not lead to significant CNC-related defects (Park et al., 2008), loss of FGF8 expression in the pharyngeal ectoderm and endoderm (Frank et al., 2002), or interfering with FGF signaling in the second heart field (SHF) mesoderm (Park et al., 2008) are sufficient to disrupt NC contribution to the heart in mouse.

The zebrafish heart originates from the fusion of bilaterally positioned primordia at the midline, which then elongates into a tubular structure (Glickman and Yelon, 2002). Cardiac progenitor cells from the SHF subsequently contribute to the developing heart through the poles. By 2 days post fertilization, the arterial half of the ventricle is primarily descended from the SHF (de Pater et al., 2009; Zhou et al., 2011). These morphogenic events are very similar to those observed in other vertebrates. In contrast, NC contribution to the developing zebrafish heart shows many unique features. Early lineage mapping analyses revealed that zebrafish CNC cells originate between rhombomere 1 and the 6th somite, a region significantly broader than those observed in chick and mouse (Sato and Yost, 2003). Interestingly, some of these cells directly contribute to the myocardium (Li et al., 2003; Sato and Yost, 2003; Mongera et al., 2013). This feature has not been noted in other vertebrates and the precise time and location of NC integration as well as the significance of these NC-derived cardiomyocytes in heart development have not been described. Furthermore, CNC cells participate in the formation of the septal complex of the OFT and gives rise to smooth muscle cells surrounding the distal portion of OFT in birds and mammals (Kirby et al., 1983; Jiang et al., 2000). The fish has a single-loop circulatory system and thus does not require OFT septation. Whether and to what extent CNC cells contribute to OFT development in fish awaits further investigation.

In this study, we generated transgenic lines to facilitate lineage tracing and found that NC contributed to the cardiovascular system at two distinct developmental stages. A stream of NC cells migrating through pharyngeal arches 1 and 2 integrates into the heart tube and adopts a myocardial fate between 24 and 30 hours post fertilization (hpf). Not until 50 hours later does a second wave of NC cells, primarily migrating along the 6th pharyngeal arch artery, surround the ventral aorta and invade bulbus arteriosus. The two waves of NC cells show disparate responses to FGF signaling; inhibiting FGF signaling does not affect the integration of NC cells to the primitive heart tube, but does abolish NC contribution to the OFT, indicating a conserved regulatory circuit in OFT development. Furthermore, NC ablation leads to defects in myocardial maturation and prevents recruitment of cardiac progenitors from the SHF.

Materials and Methods

Transgenic construct

Transgenic lines were created using the Tol2kit system (Kwan et al., 2007). For the *sox10:GAL4,UAS:Cre* construct, the *sox10* promoter (−5kb) (Carney et al., 2006) was amplified from zebrafish genomic DNA and cloned into the 5' Gateway entry vector (p5E) along with *GAL4*. *UAS:Cre-pA* was cloned into the middle entry vector pME. These entry clones and the 3' entry vector (p3E) containing BFPpA were subjected to the multisite recombination reaction to the pDestTol2pA2 destination vector by LR clonase II Plus (Life Technologies, Carlsbad, CA) to generate the transgene construct flanked by Tol2 sites.

In situ hybridization

Embryos for in situ hybridization were raised in embryo medium (5 mM NaCl, 0.17 mM KCl, 0.33 mM CaCl2, 0.33 mM MgSO4) supplemented with 0.2 mM 1-phenyl-2-thiourea to maintain optical transparency. Whole-mount in situ hybridization was performed as described previously (Chen and Fishman, 1996). The antisense RNA probes used in this study include *ltbp3* (Kindly provided by J. Burns) (Zhou et al., 2011) and *tbx2b* (Chi et al., 2008).

Antibody staining

Embryos were fixed in 4% PFA in PBS at 80 hpf. The fixed embryos were permeabilized with acetone for 5 min at room temperature, incubated in 1:1000 mouse anti-α-actinin antibody (Sigma-Aldrich, St. Louis, MO) or 1:150 zn8 antibody (Developmental Studies Hybridoma Bank, Iowa City, IA) in blocking solution (20mg/mL BSA in PBDT) overnight at 4 °C followed by detection with 1:150 goat anti-mouse IgG1-Alexa Fluor 647 antibody (Life Technologies, Carlsbad, CA).

Imaging

Embryos were fixed in 4% PFA and embedded in 1% agarose for whole mount images, or embedded in 4% low melting agarose and cut into 100 μm sections with a Leica VT1000S vibratome for tracing NC cells at early stages of heart development (Langenbacher et al., 2012). Confocal images were acquired using a Carl Zeiss Laser Scanning Systems LSM510 equipped with 20x water or 63x water immersion objectives. Images were analyzed using the Zeiss LSM Image Browser version4, Zen 2009, and Image J.

Nitroreductase mediated ablation

Embryos were soaked in 10mM metronidazole (Mtz) in embryo medium from 4 to 48 hpf (Pisharath and Parsons, 2009). The extent of NC ablation was assessed by the loss of mCherry positive cells in the heart at 48 hpf. For each experiment, untreated siblings and Mtz-treated *UAS:NfsB-mCherry (−)* embryos served as controls.

Kaede conversion

Photoconversion was achieved by exposing embryos double transgenic for *NC:NfsB-mCherry* and *myl7:kaede* (kindly provided by D. Yelon) to UV light at 26 hpf on a Zeiss

Axioplan microscope equipped with a DAPI filter set until there was a strong red signal and no detectable green fluorescence remained (Hatta et al., 2006). Embryos were then treated with Mtz from 4-48 hpf to ablate NC cells. NC-ablated embryos with reduced ventricle size were selected and fixed at 60 hpf for confocal imaging using a LSM 700 Imager M2 equipped with 40x water objective.

Chemical treatment

SU5402 (Sigma-Aldrich, St. Louis, MO) was diluted to a working concentration of 5 μM in embryo medium. Up to 10 embryos per well of a 24-well plate were treated for discrete periods of time in the dark at 28.5°C (Marques et al., 2008). After treatment, embryos were washed three times in embryo medium and raised in new plates with fresh embryo medium for analysis at 60 and 96 hpf. Control embryos were treated with a corresponding dilution of DMSO in embryo medium.

Cardiovascular measurements

Myocardial cells were counted using *myl7:nucGFP* to visualize the nuclei of each cardiomyocytes. Cells that are positive for both mCherry and nucGFP in the *NC:mCherry; myl7:nucGFP* background are considered to be NC-derived myocardial cells. Counts were performed manually with the assistance of ImageJ cell counter software.

For ventricle length, the distance from the apex of the ventricle to the bottom of the OFT was measured using the Zeiss LSM Image Browser version4 software.

To assess the shape of cardiomyocytes, plasma membrane was visualized by Zn8 staining and the longest and shortest axes of each cell were measured using Zeiss LSM Image Browser version4 software. The ratio of elongation was obtained by dividing the length of the longest axis by the length of the shortest axis.

To determine the NC coverage of the ventral aorta, the length of the ventral aorta surrounded by mCherry positive cells was measured and divided by the total length of the ventral aorta.

Statistical analysis

All values are expressed as mean and standard deviation. Significance values are calculated by unpaired student's *t*-test.

Results

Generation of Sox10 neural crest tracing lines

A ~5kb NC-specific *sox10* promoter was previously reported to faithfully recapitulate the endogenous *sox10* expression in NC cells. We fused this promoter to GAL4 and UAS-Cre (Fig. 1A) (Dutton et al., 2001; Carney et al., 2006; Kwak et al., 2013; Mongera et al., 2013) and generated two stable transgenic lines, *Tg(NC:NfsB-mCherry)* and *Tg(NC:mCherry)* (Fig. 1A).

NC:NfsB-mCherry is double transgenic for *sox10:GAL4-UAS-Cre* and *UAS:NfsB-mCherry* (Davison et al., 2007), in which the expression of Nitroreductase-mCherry fusion protein is controlled by *sox10*-driven GAL4 activity allowing lineage tracing (by mCherry) and chemical-induced cell ablation (via Nitroreductase activity) (Davison et al., 2007). We detected mCherry positive NCCs in *NC:NfsB-mCherry* embryos as early as the 16-somite stage (ss) and observed a significant number of mCherry-labeled NC cells in the developing head and in the trunk by 20ss (Fig. 1B), consistent with the reported *sox10* expression pattern (Dutton et al., 2001; Carney et al., 2006; Kwak et al., 2013; Mongera et al., 2013). In addition, mCherry positive NC-derived cells were detected in the developing heart (Figs. 2, 3), confirming previous reports that some NC-derived cells contribute to the zebrafish heart (Li et al., 2003; Sato and Yost, 2003; Kague et al., 2012; Mongera et al., 2013; Xia et al., 2013).

As development proceeds, *sox10* transcription is reduced and mCherry signal in *NC:NfsB-mCherry* diminishes, preventing the analysis of CNC contribution at later developmental stages. To overcome this problem, we generated *Tg(NC:mCherry)*, a double transgenic line for the *sox10:GAL4-UAS-Cre* transgene and the *ubi:Switch* reporter (Fig. 1A) (Mosimann et al., 2011). In *NC:mCherry*, *sox10* promoter drives the expression of Cre recombinase in NC cells which excises GFP and permanently labels cells of *sox10* lineage with mCherry. By 108 hpf, mCherry positive cells were observed in all known NC-derived tissues, including most elements of the craniofacial skeleton as previously reported (Fig. 1C) (Kague et al., 2012), as well as the heart (Figs. 2, 3) and the OFT (Fig. 4). Together *NC:NfsB-mCherry* and *NC:mCherry* transgenic fish allow for tracing of NC-derived cells in the cardiovascular system from early embryonic stages to adulthood. In this study, we used *NC:NfsB-mCherry* to examine NC contribution to the developing heart in the first 3 days of development and used *NC:mCherry* for the analysis at later developmental stages.

Neural crest cells differentiate into cardiomyocytes

To determine the timing of NC contribution to the heart and whether these cells adopt a cardiac fate, we crossed *NC:NfsB-mCherry* to *myl7:nucGFP*, a reporter line in which myocardial cells express nuclear GFP. At 17 hpf, a small number of NC cells migrating through pharyngeal arches 1 and 2 began to approach the bilaterally positioned cardiac precursors (Fig. 2A-C). When cardiac precursors merge at the midline, more NC cells came in close proximity to the heart (Fig. 2D-F). However, not until 24 hpf when the heart tube elongates and jogs to the left did we begin to observe the integration of NC-derived cells into the heart. These cells soon became positive for nuclear GFP, indicating that they had adopted a myocardial fate (Fig. 2H-J, Supplemental Video 1).

We observed active NC contribution along the primitive heart tube without apparent bias between the atrium and ventricle from 24 to 30 hpf (Figs. 2G-G'' and 3A-A''). Addition of NC cells to the developing heart tube ceased around 30 hpf and the number of mCherry positive cells in the heart remained static to 78 hpf (23 ± 6.67 NC-derived cells in the heart at 30 hpf, n=9, 19 ± 8.13 at 60 hpf, n=5 and 19 ± 6.03 at 78 hpf, n=6; *p*=0.28) (Fig 3E). As cardiac progenitors from the SHF add to the developing heart from both poles, the percentage of NC-derived cardiomyocytes per heart decreased (12.19%, at 30 hpf to 8.35%

at 60 hpf and 7.57% at 78 hpf) (Fig.3E), and the NC-derived cardiomyocytes became more restricted to the base of the ventricle, AV boundary, and the proximal atrium after two days of development (Fig 3B-C'', F) (de Pater et al., 2009; Lazic and Scott, 2011; Zhou et al., 2011). Immunostaining using anti-alpha actinin antibody showed that NC-derived cardiomyocytes have organized z-lines as do other cardiomyocytes (Fig.3D-D'''), indicating that these cells are contractile.

Neural crest cells contribute to the ventral aorta and bulbus arteriosus

Using the *NC:mCherry* fish, we found that NC-derived cells enveloped the endothelium of the ventral aorta (VA) and invaded the bulbus arteriosus (BA) around 80 hpf, approximately 50 hours after NC cells finished contributing to the heart tube. To better examine this process, we crossed *Tg(NC:NfsB-mCherry)* and *Tg(NC:mCherry)* into the *kdrl:GFP* transgenic line, in which endothelial cells are marked by GFP (Choi et al., 2007). At 60 hpf, the VA is very short and the BA is small (Fig.4A). At this stage, a few mCherry positive NC cells began to migrate out of the 6th aortic arch artery toward the heart along the endothelium of the VA (Fig. 4A-A''). By 80 hpf, when the VA has elongated and the BA becomes more pronounced, mCherry positive cells began to encircle the endothelium of VA (Fig. 4B-B''). At 108 hpf, the endothelial layer of the VA was fully surrounded by NC-derived cells and a small number of NC-derived cells began to populate the BA (Fig. 4C-C''), resembling the pattern observed in other vertebrate models (Kirby et al., 1983; Jiang et al., 2000; Lee and Saint-Jeannet, 2011).

Cardiac neural crest contribution to the outflow tract requires FGF signaling

FGF signaling interacts extensively with NC cells in the pharyngeal arches (David et al., 2002; Frank et al., 2002; Nissen et al., 2003; Crump et al., 2004; Sato et al., 2011). To determine the impact of FGF signaling on NC contribution to the cardiovascular system, we treated *NC:NfsB-mCherry* and *NC:mCherry* embryos with SU5402, a potent inhibitor of fibroblast growth factor receptor (FGFR), from 16 hpf to 48 hpf (Mohammadi et al., 1997) (Fig. 5A). Consistent with previous reports, embryos treated with SU5402 were deformed with a shorter, curved body and diminutive ventricle (Fig. S1) (David et al., 2002; Nissen et al., 2003; Crump et al., 2004; Marques et al., 2008). Interestingly, even though the SU5402-treated hearts became dysmorphic, NC cells still integrated into the heart and adopted a myocardial fate (15.5±5.4 in DMSO-treated control embryos, n=4 *versus* 18.5±1.5 in SU5402-treated embryos, n=6, p = 0.23) (Fig. 5E-F'').

The pharyngeal vasculature and VA were severely defective in embryos subjected to extended SU5402 treatment (16-48, 30-48 and 36-48 hpf), preventing the assessment of NC contribution (Fig.S1). We thus treated *NC:mCherry* embryos with SU5402 from 42 hpf until 48 hpf. Embryos subjected to this shortened treatment have intact pharyngeal vasculature, but the length of the VA surrounded by NC-derived cells was severely reduced (97.6±5.4% in DMSO-treated control embryos, n=5 *versus* 56.3±16.2% in SU5402-treated embryos, n=10, p<0.001) (Fig. 5A-D''). These findings demonstrate a differential requirement for FGF signaling in NC contribution to the heart and the OFT; FGF signals are required for the contribution of NC cells to the VA and BA but are dispensable for those contributing the cardiac chambers.

Neural crest ablation perturbs cardiac function and morphology

Nitroreductase converts the pro-drug metronidazole (Mtz) to a toxic form (Pisharath and Parsons, 2009). In *NC:NfsB-mCherry* embryos, the *sox10* promoter drives the production of Nitroreductase in NC cells allowing the ablation of *NfsB-mCherry* positive cells. *NC:NfsB-mCherry* embryos treated with Mtz showed a nearly complete absence of mCherry positive cells in the heart (Fig. 6A-B'') as well as a reduction in pigment and defects in craniofacial development (data not shown); a phenotype consistent with the loss of NC cells (Dutton et al., 2001).

NC ablation did not appear to affect the formation of the primitive heart tube, but the heart rate of NC-ablated embryos became depressed by 33 hpf (89.09 ± 6.07 beat per minute in control *versus* 81.49 ± 7.40 in NC-ablated embryos, n=10 each, $p<0.05$) (Fig. 6C). After two days of development, the ventricle of NC-ablated embryos was significantly smaller (ventricle length: 111.93 ± 4.91 μm in control *versus* 96.22 ± 4.28 μm in NC-ablated embryos, n=6 each, $p<0.001$) and had a reduced number of myocardial cells (123.75 ± 12.76 in control embryos *versus* 90.75 ± 5.91 in NC-ablated embryos, n=4 each, $p<0.05$) (Fig. 6A-B'', D). The differentiation of the AV boundary was also defective as evident in the expanded expression domain of *tbx2b* (Fig. 6E-F) (Chi et al., 2008). Normally, zebrafish ventricular cardiomyocytes undergo characteristic cell shape changes as they mature, with myocardial cells in the outer curvature elongating to assume a more wedge shape, while cells closer to the AV canal maintain a more cuboidal morphology (Fig. 6G-G') (Auman et al., 2007). In NC-ablated embryos, myocardial cells in both the outer and inner curvature maintain a cuboidal morphology (Fig. 6H-H') and the differences between outer and inner curvature cells were lost (axis ratio of outer curvature cardiomyocytes: 2.49 ± 0.09 in control and 1.75 ± 0.22 in NC-ablated embryos, p = 0.006; axis ratio of inner curvature cardiomyocytes: 1.66 ± 0.11 in control and 1.70 ± 0.16 in NC-ablated embryos, n=4 each, p = 0.77) (Fig. 6I), indicating myocardial maturation defects.

Neural crest ablation abolishes the recruitment of cells from the SHF

NC-derived cardiomyocytes account for about 10% of total cardiomyocytes in 2-day-old embryonic hearts (Fig.3D), but there was an approximately 27% reduction of ventricular cardiomyocytes in NC-ablated embryos (123.75 ± 12.76 in control *versus* 90.75 ± 5.91 in NC-ablated embryos, $p<0.05$; Fig.6D). In zebrafish, cardiac progenitor cells from the SHF are added to the primitive heart tube from both poles and loss of SHF contribution results in a small ventricle (de Pater et al., 2009; Witzel et al., 2012). Studies in chick and mouse have also observed an association between NC defects and the recruitment of OFT myocardium from the SHF (Bradshaw et al., 2009; Zhou et al., 2011). We thus examined whether the small ventricle phenotype observed in NC-ablated embryos was due to SHF defects. *Ltbp3* is a well-characterized SHF marker whose expression is quickly downregulated as SHF cardiac progenitor cells differentiate and migrate into the heart (Zhou et al., 2011). At 24 hpf, *ltbp3* expression was comparable between control and NC-ablated embryos, demonstrating that NC cells are not required for SHF specification. Interestingly, by the time when *ltbp3* expression was diminished in control embryos, its expression persisted in NC-ablated embryos (Fig. 7A, B), raising an intriguing possibility that SHF cardiac progenitors fail to differentiate and contribute to the heart.

To further evaluate the extent of SHF contribution to NC-ablated hearts, we took the advantage of the *myl7:kaede* fish in which photoconvertible Kaede is expressed specifically in cardiomyocytes (de Pater et al., 2009). We photoconverted the Kaede protein from green to red in the heart tube at 26 hpf. By 60 hpf, the arterial end of the ventricle in control embryos was marked by green fluorescing Kaede alone (11/11 embryos imaged), whereas the entire ventricle of NC-ablated embryos was marked by red fluorescing Kaede (14/16 NC-ablated embryos imaged) (Fig. 7C-D''), demonstrating a loss of SHF contribution to the heart.

Discussion

The contribution of NC cells to the myocardium of the zebrafish heart has been noted for more than a decade (Li et al., 2003; Sato and Yost, 2003). However, the precise timing of the integration of NC-derived cells and the requirement of these cells for heart development and function are largely unknown. In this study we created two transgenic lines using GAL4-UAS and cre-lox labeling systems to investigate NC contribution to the zebrafish heart. We show that NC cells contribute to two distinct compartments of the zebrafish cardiovascular system at different developmental stages. A stream of NC cells integrates into the primitive heart tube between 24 and 30 hpf and adopts a myocardial fate. Another wave of NC cells migrating off of aortic arch 6 surrounds the endothelium of the VA and populates the BA by 108 hpf. Interestingly, these two populations of NC cells show disparate responses to FGF signaling; the first-wave of CNC cells do not require FGF signaling whereas the second-wave CNC cells populate the OFT in an FGF-dependent manner. Furthermore, we assessed the NC requirement for in cardiac development and observed defects in myocardial maturation and cardiac function in NC-ablated embryos.

In addition to the septation complex, NC cells give rise to the smooth muscle layer of the distal portion of OFT in chick and mouse models (Topouzis and Majesky, 1996; Jiang et al., 2000). The contribution of NC cells to the great vessels leading out of the heart had not been examined in zebrafish, in part due to the need of genetic tools to trace these cells. Using *NC:mCherry*, we permanently marked *sox10* positive NC cells with mCherry and observed a previously unappreciated NC population. These cells migrate along aortic arch artery 6 in response to FGF signaling and envelop the endothelium of the VA and the distal portion of the BA by 4 dpf, a timing similar to the appearance of a*cta2-* and *transgenlin/SM22*-positive mural cells in the VA (Santoro et al., 2009; Whitesell et al., 2014). The observation that ablating a NC population by FoxD3 and TFAP2 mopholinos reduced the mural cell coverage in the VA raises an intriguing possibility that mural cells in the OFT are of NC origin (Whitesell et al., 2014). Future investigation on whether and at what stages the *sox10* positive NC-derived cells differentiate into smooth muscles in the zebrafish will provide new insights into how NC cells involved in zebrafish OFT development.

NC cells are pluripotent and differentiate to a wide variety of cell types. Their contribution to the myocardial layer has long been noted in fish (Li et al., 2003; Sato and Yost, 2003), but the precise timing of when these cells contribute to the heart and the distribution of these cells in the zebrafish heart have been elusive. In this study, we used the GAL4-UAS system to drive strong mCherry signals in *sox10* expressing cells and found that NC-derived cells

integrate into the myocardial layer along the entire primitive heart tube and adopt a myocardial fate between 24 and 30 hpf. The static number of NC-derived cardiomyocytes during the first three days of development is consistent with the relatively low proliferation of cardiomyocyotes during this period of time (Choi et al., 2013). After the addition of SHF-derived cardiomyocytes, NC-derived cardiomyocytes become restricted to the middle section of the heart, suggesting that these cells do not migrate extensively once they integrate into the heart tube. These cells differ from those CNC cells characterized in chick and mouse in that they originate from a broader range of embryonic tissues (Sato and Yost, 2003), migrate through more anterior pharyngeal arches (I and II) (Fig.2) and do not require FGF signaling (Fig.5). It is interesting to note that lineage studies using the PO1 promoter in mice detected a small population of undifferentiated NC-derived cells nested in the myocardium of both atria and the left ventricle (Tomita et al., 2005; Tamura et al., 2011). These PO-1 derived cells have the potential to differentiate into cardiomyocytes upon injury and they are excluded from the SHF-derived right ventricle, echoing our observations in zebrafish (Tomita et al., 2005; Tamura et al., 2011). It would be of great interest to evaluate whether the PO1-derived NC cells represent a mammalian counterpart to NC-derived myocardial cells observed in the fish model.

NC-ablation results in a slower heart rate and a loss of the SHF-derived cardiomyocytes in the ventricle. The persistent expression of *ltbp3* in NC-ablated fish embryos suggests that the SHF mesoderm failed to differentiate into the myocardial fate in the absence of neural crest cells. This phenotype resembles the defect in recruiting SHF-derived myocardium to OFT in mouse and chick NC-deficient models (Yelbuz et al., 2002; Waldo et al., 2005; Hutson et al., 2006). Elevated FGF8 signaling was observed in CNC-ablated chick embryos and blocking FGF signaling was sufficient to restore the OFT myocardium (Hutson et al., 2006), suggesting that these defects are in part mediated by FGF signaling in the pharynx. It would be of great interest to evaluate whether similar signaling events between CNC cells and the SHF mesoderm also govern zebrafish heart development. Furthermore, the expanded *tbx2b* expression domain at the AV boundary and the failure of outer curvature cardiomyocytes to assume a characteristic wedge shape indicate defects in the maturation of the myocardium (Auman et al., 2007; Chi et al., 2008). Future studies on whether NC cells directly regulate the differentiation of the AV boundary and the remodeling of the developing ventricle would provide new insights into the biological requirement of NC cells in heart development.

Supplementary Material

Refer to Web version on PubMed Central for supplementary material.

Acknowledgements

References

Abu-Issa R, Smyth G, Smoak I, Yamamura K, Meyers EN. Fgf8 is required for pharyngeal arch and cardiovascular development in the mouse. Development (Cambridge, England). 2002; 129:4613–4625.

Auman HJ, Coleman H, Riley HE, Olale F, Tsai HJ, Yelon D. Functional modulation of cardiac form through regionally confined cell shape changes. PLoS biology. 2007; 5:e53. [PubMed: 17311471]

Besson WT, Kirby ML, Van Mierop LH, Teabeaut JR. Effects of the size of lesions of the cardiac neural crest at various embryonic ages on incidence and type of cardiac defects. Circulation. 1986; 73:360–364. [PubMed: 3943168]

Bradshaw L, Chaudhry B, Hildreth V, Webb S, Henderson DJ. Dual role for neural crest cells during outflow tract septation in the neural crest-deficient mutant Splotch(2H). Journal of anatomy. 2009; 214:245–257. [PubMed: 19207986]

Carney TJ, Dutton KA, Greenhill E, Delfino-Machin M, Dufourcq P, Blader P, Kelsh RN. A direct role for Sox10 in specification of neural crest-derived sensory neurons. Development. 2006; 133:4619–4630. [PubMed: 17065232]

Chen JN, Fishman MC. Zebrafish tinman homolog demarcates the heart field and initiates myocardial differentiation. Development. 1996; 122:3809–3816. [PubMed: 9012502]

Chi NC, Shaw RM, De Val S, Kang G, Jan LY, Black BL, Stainier DY. Foxn4 directly regulates tbx2b expression and atrioventricular canal formation. Genes & development. 2008; 22:734–739. [PubMed: 18347092]

Choi J, Dong L, Ahn J, Dao D, Hammerschmidt M, Chen JN. FoxH1 negatively modulates flk1 gene expression and vascular formation in zebrafish. Developmental biology. 2007; 304:735–744. [PubMed: 17306248]

Choi WY, Gemberling M, Wang J, Holdway JE, Shen MC, Karlstrom RO, Poss KD. In vivo monitoring of cardiomyocyte proliferation to identify chemical modifiers of heart regeneration. Development. 2013; 140:660–666. [PubMed: 23293297]

Conway SJ, Henderson DJ, Kirby ML, Anderson RH, Copp AJ. Development of a lethal congenital heart defect in the splotch (Pax3) mutant mouse. Cardiovascular research. 1997; 36:163–173. [PubMed: 9463628]

Crump JG, Swartz ME, Kimmel CB. An integrin-dependent role of pouch endoderm in hyoid cartilage development. PLoS biology. 2004; 2:E244. [PubMed: 15269787]

David NB, Saint-Etienne L, Tsang M, Schilling TF, Rosa FM. Requirement for endoderm and FGF3 in ventral head skeleton formation. Development. 2002; 129:4457–4468. [PubMed: 12223404]

Davison JM, Akitake CM, Goll MG, Rhee JM, Gosse N, Baier H, Halpern ME, Leach SD, Parsons MJ. Transactivation from Gal4-VP16 transgenic insertions for tissue-specific cell labeling and ablation in zebrafish. Developmental biology. 2007; 304:811–824. [PubMed: 17335798]

de Pater E, Clijsters L, Marques SR, Lin YF, Garavito-Aguilar ZV, Yelon D, Bakkers J. Distinct phases of cardiomyocyte differentiation regulate growth of the zebrafish heart. Development. 2009; 136:1633–1641. [PubMed: 19395641]

Dutton KA, Pauliny A, Lopes SS, Elworthy S, Carney TJ, Rauch J, Geisler R, Haffter P, Kelsh RN. Zebrafish colourless encodes sox10 and specifies non-ectomesenchymal neural crest fates. Development. 2001; 128:4113–4125. [PubMed: 11684650]

Frank DU, Fotheringham LK, Brewer JA, Muglia LJ, Tristani-Firouzi M, Capecchi MR, Moon AM. An Fgf8 mouse mutant phenocopies human 22q11 deletion syndrome. Development. 2002; 129:4591–4603. [PubMed: 12223415]

Glickman NS, Yelon D. Cardiac development in zebrafish: coordination of form and function. Seminars in cell & developmental biology. 2002; 13:507–513. [PubMed: 12468254]

Hatta K, Tsujii H, Omura T. Cell tracking using a photoconvertible fluorescent protein. Nature protocols. 2006; 1:960–967. [PubMed: 17406330]

Hutson MR, Kirby ML. Neural crest and cardiovascular development: A 20-year perspective. Birth Defects Research Part C: Embryo Today: Reviews. 2003; 69:2–13.

Hutson MR, Zhang P, Stadt HA, Sato AK, Li YX, Burch J, Creazzo TL, Kirby ML. Cardiac arterial pole alignment is sensitive to FGF8 signaling in the pharynx. Developmental biology. 2006; 295:486–497. [PubMed: 16765936]

Jiang X, Rowitch DH, Soriano P, McMahon AP, Sucov HM. Fate of the mammalian cardiac neural crest. Development. 2000; 127:1607–1616. [PubMed: 10725237]

Kague E, Gallagher M, Burke S, Parsons M, Franz-Odendaal T, Fisher S. Skeletogenic fate of zebrafish cranial and trunk neural crest. PloS one. 2012; 7:e47394. [PubMed: 23155370]

Kirby ML, Gale TF, Stewart DE. Neural crest cells contribute to normal aorticopulmonary septation. Science (New York, N.Y.). 1983; 220:1059–1061.

Kwak J, Park OK, Jung YJ, Hwang BJ, Kwon SH, Kee Y. Live image profiling of neural crest lineages in zebrafish transgenic lines. Molecules and cells. 2013; 35:255–260. [PubMed: 23456294]

Kwan KM, Fujimoto E, Grabher C, Mangum BD, Hardy ME, Campbell DS, Parant JM, Yost HJ, Kanki JP, Chien CB. The Tol2kit: a multisite gateway-based construction kit for Tol2 transposon transgenesis constructs. Developmental dynamics : an official publication of the American Association of Anatomists. 2007; 236:3088–3099. [PubMed: 17937395]

Langenbacher AD, Huang J, Chen Y, Chen JN. Sodium pump activity in the yolk syncytial layer regulates zebrafish heart tube morphogenesis. Developmental biology. 2012; 362:263–270. [PubMed: 22182522]

Lazic S, Scott IC. Mef2cb regulates late myocardial cell addition from a second heart field-like population of progenitors in zebrafish. Developmental biology. 2011; 354:123–133. [PubMed: 21466801]

Le Douarin, N.; Kalcheim, C. The neural crest. Cambridge University Press; 1999.

Lee YH, Saint-Jeannet JP. Cardiac neural crest is dispensable for outflow tract septation in Xenopus. Development. 2011; 138:2025–2034. [PubMed: 21490068]

Li YX, Zdanowicz M, Young L, Kumiski D, Leatherbury L, Kirby ML. Cardiac neural crest in zebrafish embryos contributes to myocardial cell lineage and early heart function. Developmental dynamics : an official publication of the American Association of Anatomists. 2003; 226:540–550. [PubMed: 12619138]

Marques SR, Lee Y, Poss KD, Yelon D. Reiterative roles for FGF signaling in the establishment of size and proportion of the zebrafish heart. Developmental biology. 2008; 321:397–406. [PubMed: 18639539]

Mohammadi M, McMahon G, Sun L, Tang C, Hirth P, Yeh BK, Hubbard SR, Schlessinger J. Structures of the tyrosine kinase domain of fibroblast growth factor receptor in complex with inhibitors. Science (New York, N.Y.). 1997; 276:955–960.

Mongera A, Singh AP, Levesque MP, Chen YY, Konstantinidis P, Nusslein-Volhard C. Genetic lineage labeling in zebrafish uncovers novel neural crest contributions to the head, including gill pillar cells. Development. 2013; 140:916–925. [PubMed: 23362350]

Mosimann C, Kaufman CK, Li P, Pugach EK, Tamplin OJ, Zon LI. Ubiquitous transgene expression and Cre-based recombination driven by the ubiquitin promoter in zebrafish. Development. 2011; 138:169–177. [PubMed: 21138979]

Nissen RM, Yan J, Amsterdam A, Hopkins N, Burgess SM. Zebrafish foxi one modulates cellular responses to Fgf signaling required for the integrity of ear and jaw patterning. Development. 2003; 130:2543–2554. [PubMed: 12702667]

Park EJ, Watanabe Y, Smyth G, Miyagawa-Tomita S, Meyers E, Klingensmith J, Camenisch T, Buckingham M, Moon AM. An FGF autocrine loop initiated in second heart field mesoderm regulates morphogenesis at the arterial pole of the heart. Development. 2008; 135:3599–3610. [PubMed: 18832392]

Pisharath H, Parsons MJ. Nitroreductase-mediated cell ablation in transgenic zebrafish embryos. Methods in molecular biology (Clifton, N.J.). 2009; 546:133–143.

Santoro MM, Pesce G, Stainier DY. Characterization of vascular mural cells during zebrafish development. Mechanisms of development. 2009; 126:638–649. [PubMed: 19539756]

Sato A, Scholl AM, Kuhn EN, Stadt HA, Decker JR, Pegram K, Hutson MR, Kirby ML. FGF8 signaling is chemotactic for cardiac neural crest cells. Developmental biology. 2011; 354:18–30. [PubMed: 21419761]

Sato M, Yost HJ. Cardiac neural crest contributes to cardiomyogenesis in zebrafish. Developmental biology. 2003; 257:127–139. [PubMed: 12710962]

Tamura Y, Matsumura K, Sano M, Tabata H, Kimura K, Ieda M, Arai T, Ohno Y, Kanazawa H, Yuasa S, Kaneda R, Makino S, Nakajima K, Okano H, Fukuda K. Neural crest-derived stem cells migrate and differentiate into cardiomyocytes after myocardial infarction. Arteriosclerosis, thrombosis, and vascular biology. 2011; 31:582–589.

Targoff KL, Colombo S, George V, Schell T, Kim SH, Solnica-Krezel L, Yelon D. Nkx genes are essential for maintenance of ventricular identity. Development. 2013; 140:4203–4213. [PubMed: 24026123]

Tomita Y, Matsumura K, Wakamatsu Y, Matsuzaki Y, Shibuya I, Kawaguchi H, Ieda M, Kanakubo S, Shimazaki T, Ogawa S, Osumi N, Okano H, Fukuda K. Cardiac neural crest cells contribute to the dormant multipotent stem cell in the mammalian heart. The Journal of cell biology. 2005; 170:1135–1146. [PubMed: 16186259]

Topouzis S, Majesky MW. Smooth muscle lineage diversity in the chick embryo. Two types of aortic smooth muscle cell differ in growth and receptor-mediated transcriptional responses to transforming growth factor-beta. Developmental biology. 1996; 178:430–445.

Waldo KL, Hutson MR, Stadt HA, Zdanowicz M, Zdanowicz J, Kirby ML. Cardiac neural crest is necessary for normal addition of the myocardium to the arterial pole from the secondary heart field. Developmental biology. 2005; 281:66–77. [PubMed: 15848389]

Whitesell TR, Kennedy RM, Carter AD, Rollins EL, Georgijevic S, Santoro MM, Childs SJ. An alpha-smooth muscle actin (acta2/alphasma) zebrafish transgenic line marking vascular mural cells and visceral smooth muscle cells. PloS one. 2014; 9:e90590. [PubMed: 24594685]

Witzel HR, Jungblut B, Choe CP, Crump JG, Braun T, Dobreva G. The LIM protein Ajuba restricts the second heart field progenitor pool by regulating Isl1 activity. Developmental cell. 2012; 23:58–70. [PubMed: 22771034]

Xia Z, Tong X, Liang F, Zhang Y, Kuok C, Zhang Y, Liu X, Zhu Z, Lin S, Zhang B. Eif3ba regulates cranial neural crest development by modulating p53 in zebrafish. Developmental biology. 2013; 381:83–96. [PubMed: 23791820]

Yelbuz TM, Waldo KL, Kumiski DH, Stadt HA, Wolfe RR, Leatherbury L, Kirby ML. Shortened outflow tract leads to altered cardiac looping after neural crest ablation. Circulation. 2002; 106:504–510. [PubMed: 12135953]

Zhou Y, Cashman TJ, Nevis KR, Obregon P, Carney SA, Liu Y, Gu A, Mosimann C, Sondalle S, Peterson RE, Heideman W, Burns CE, Burns CG. Latent TGF-beta binding protein 3 identifies a second heart field in zebrafish. Nature. 2011; 474:645–648. [PubMed: 21623370]

Highlights

- Neural crest cells contribute to distinct cardiovascular compartments in two waves.

- A stream of neural crest cells integrates into the primitive heart tube and adopts a myocardial fate.

- A second wave of neural crest cells encircles the ventral aorta and populates bulbus arteriosus.

- FGF signaling is dispensable for neural crest integration to the heart tube, but is instrumental to their contribution to the outflow tract.

- Neural crest ablation impairs cardiac maturation and inhibits the recruitment of second heart field progenitors.
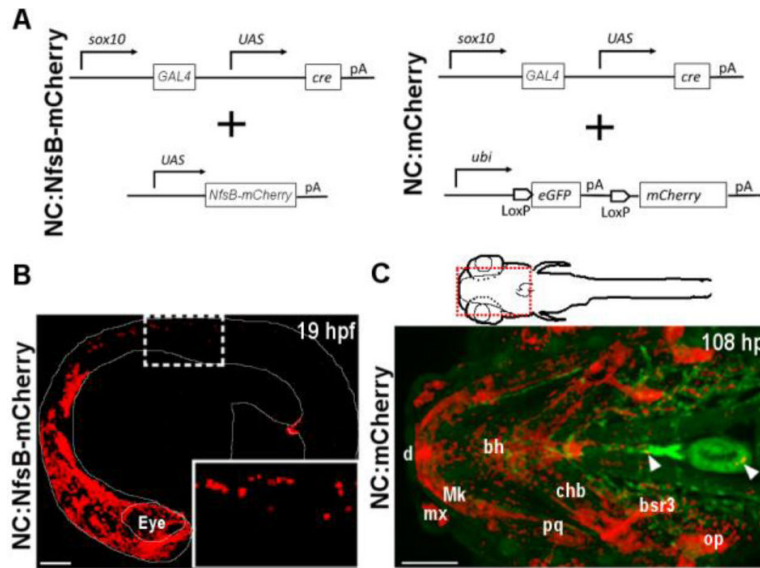
Fig. 1.

sox10 transgenic constructs and expression in zebrafish.

(A) Schematic representation of transgenic strategy used to generate *NC:NfsB-mCherry* and *NC:mCherry* lines. (B) Confocal image of *NC:NfsB-mCherry* fish at 19 hpf from a lateral view (anterior to left). The mCherry positive cells are found in cranial and trunk neural crest (box enlarged in inset). (C) Ventral view of the anterior region (indicated by red box on illustration) of *NC:mCherry; kdrl:GFP* embryo at 108 hpf (anterior to left). The mCherry positive cells are observed in craniofacial structures, as well as the heart (arrowhead) and around the ventral aorta (arrowhead). bh, basihyal; bsr3, branchiostegal ray 3; chb, ceratohyal; d, dentea; mx, maxilla; Mk, Meckel's cartilage; op, opericle; pq, palatoquadrate. Scale bars = 100 μm.
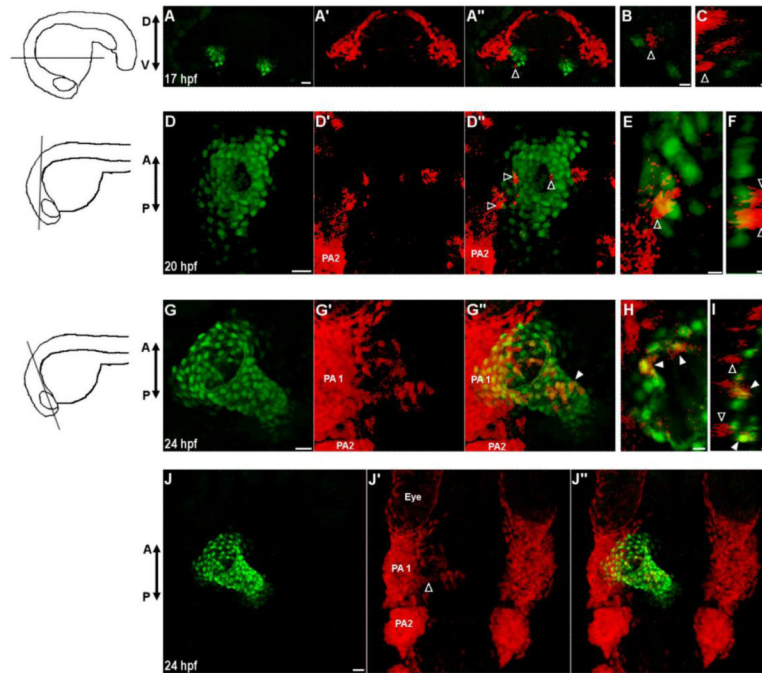
Fig. 2.
Neural crest cells contribute to the primitive heart tube.

(A-J) Confocal images of vibratome sections of *NC:NfsB-mCherry; myl7:nucGFP* embryos. Orientation of each section is indicated by illustration on the left. *Sox10* positive cells are marked by mCherry and *myl7* positive cardiomyocytes express nuclear GFP. At 17 hpf (A-C) and 20 hpf (D-F) mCherry+ cells are in close proximity of the heart and have not adopted a myocardial fate (open arrowhead). (G-I) At 24 hpf, some mCherry+ cells have integrated into the primitive heart tube and express nucGFP (closed arrowhead) while those mCherry+ cells adjacent to the heart do not (open arrowheads). (J-J'') Dorsal view of the anterior region of the same embryo in G, showing mCherry+ cells migrating out of PA1 (open arrowhead). (A,D,G,J) Confocal projections of vibrotome sections, scale bar = 20μm. (B,E,H) Single confocal section, scale bar = 5 μm. (C,F,I) Orthogonal reconstruction, scale bar = 5μm. PA1, pharyngeal arch 1; PA2, pharyngeal arch 2, D, dorsal; V, ventral; A, anterior; P, posterior.
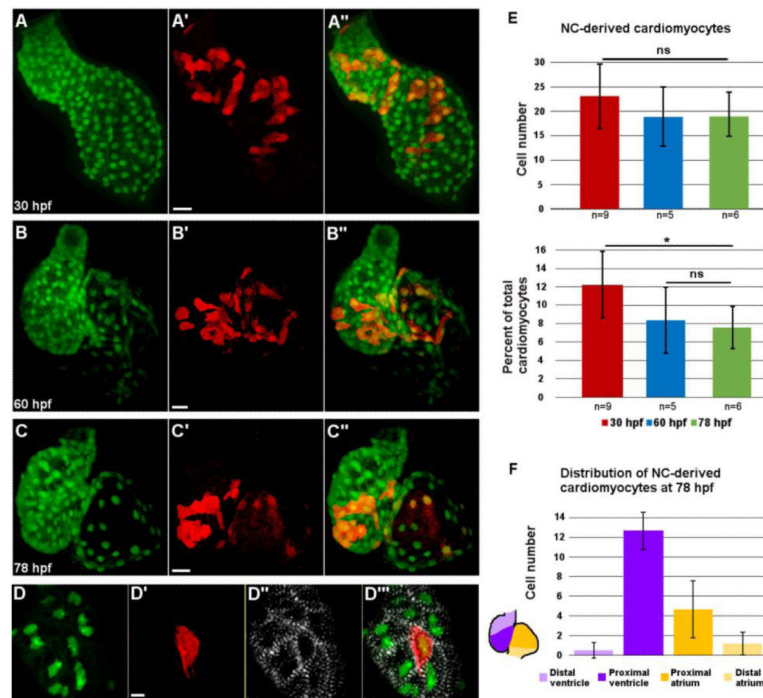
Fig. 3.
Distribution of neural crest-derived cardiomyocytes in developing zebrafish heart.
(A-C'') Confocal projections of *NC:NfsB-mCherry; myl7:nucGFP* embryonic hearts at 30
hpf (A-A''), 60 hpf (B-B''), and 78 hpf (C-C''). (A-A") NC-derived mCherry positive cells
are distributed along the primitive heart tube at 30 hpf. (B-C") As development progresses,
mCherry+ cells become excluded from the poles of the heart. Scale bar = 20 μm. (D-D''')
Confocal image of the ventricle of a *NC:NfsB-mCherry; myl7:nucGFP* embryo at 72 hpf.
Immunostaining for α-actinin (white) demonstrates well-developed sarcomeres in NC-
derived cardiomyocytes. Scale bar = 5μm. (E) Quantification of the number (top) and the
percentage (lower panel) of NC-derived cardiomyocytes (positive for both mCherry and
nucGFP) at 30 hpf, 60 hpf and 78 hpf. (F) At 78 hpf NC-derived cardiomyocytes contribute
primarily to the proximal ventricle (12.7±1.9) and proximal atrium (4.7±2.9), with very little
contribution to the distal ventricle (0.5±0.8) and distal atrium (1.2±1.5) (n=6). *, p < 0.05;
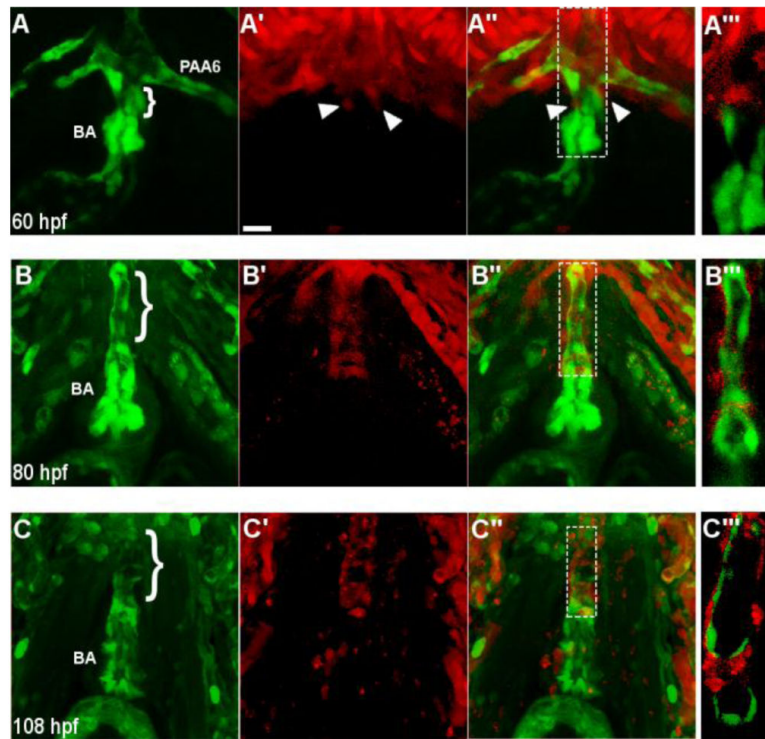ns, not significant.

Fig. 4.
Neural crest-derived cells surround the endothelium of the ventral aorta and bulbus arteriosus. (A-A'') A confocal projection of a ventral view of the BA and VA of a *NC:NfsB-mCherry; kdrl:GFP* embryo at 60 hpf (anterior toward top). Arrowheads point to neural crest cells migrating onto the VA from the 6th aortic arch artery. (B-C'') Confocal projections of BA and VA of a *NC:mCherry; kdrl:GFP* embryo at 80 hpf (B-B''') and 108 hpf (C-C''') show the progression of mCherry+ cells migrating along the VA. A''', B''' and C''', Single z section of area boxed in A'', B'' and C'', respectively. Brackets mark the ventral aorta (VA); BA, bulbus arteriosis; PAA6, pharyngeal arch artery 6, scale bar = 20μm.
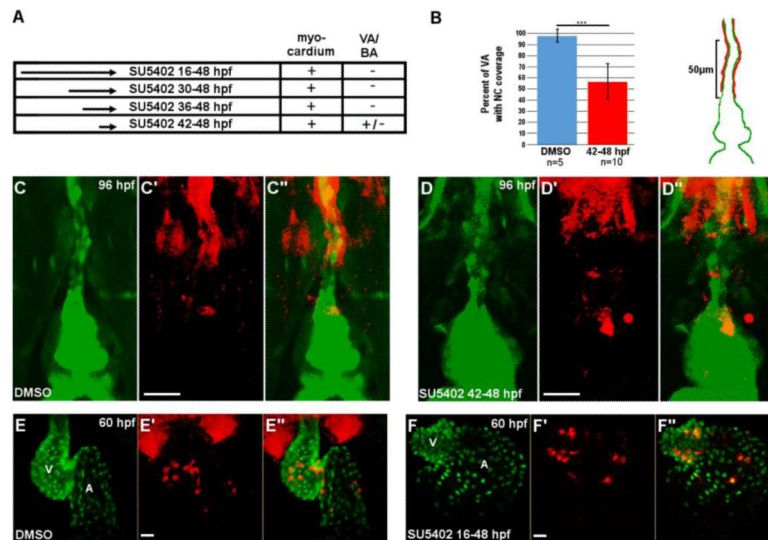
Fig. 5.
Requirement for FGF signaling in neural crest contribution to the heart.

(A) Experimental design and results for FGF inhibition using SU5402. NC contribution to cardiac chambers was not affected by FGF inhibition at any time point, while NC contribution to the VA and BA was reduced by FGF inhibition. +, mCherry cells present; -, mCherry cells absent; +/-, drastically reduced mCherry cells. (B) Percent coverage of the ventral aorta by NC-derived cells for DMSO-treated control embryos, and embryos treated with SU5402 from 42-48 hpf. Cartoon illustrates the 50μm area of the VA assessed for coverage by mCherry positive cells. Red represents mCherry cells and green represents the endothelium of the VA and BA. (C-D'') Confocal projections of the BA and VA in DMSO-treated control (C-C'') and SU5402-treated *NC:mCherry; kdrl:GFP* embryos (D-D''). (E-F'') Confocal projections of DMSO-treated control (E-E'') and SU5402-treated *NC: mCherry; myl7:GFP* embryos. VA, ventral aorta; BA, bulbus arteriosus, A, atrium; V, ventricle. Scale bars = 20μm. ***, $p < 0.001$.
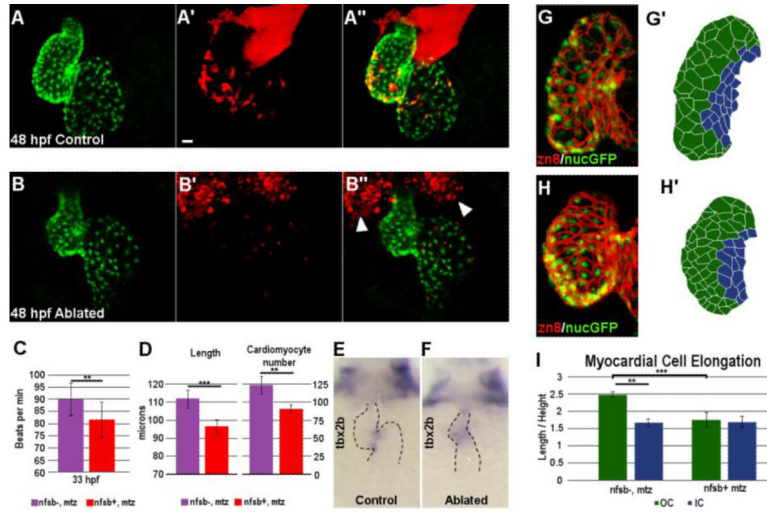
Fig. 6.
Neural crest ablation affects cardiac function and morphology.
Confocal projection of hearts from untreated control (A-A'') and Mtz-treated (B-B'')
NC:NfsB-mCherry; myl7:nucGFP embryos. Note that Mtz-treated embryos had smaller
ventricles. Arrowheads point to dying NCCs in surrounding tissues. Scale bar = 20μm. (C)
Graph indicates heart rate in Mtz-treated NfsB-mCherry (−) controls and Mtz-treated NfsB-
mCherry (+) NC-ablated embryos at 33 hpf. (D) Graph indicates ventricle length of Mtz-
treated NfsB-mCherry (−) controls and Mtz-treated NfsB-mCherry (+) NC-ablated embryos
at 48 hpf and ventricular myocardial cell number at 72 hpf. (E,F) In situ hybridization for
tbx2b at 60 hpf in control (E) and NC-ablated embryos (F). Note that *tbx2b* expression
domain is expanded in NC-ablated embryos. (G, H) Confocal projections of 80 hpf
ventricles immunostained with membrane marker Zn8 from control (G) and NC-ablated
embryos (H). (G', H') Traces of cell shape from the images shown in G and H with outer
curvature cells in green and inner curvature cells in blue. (I) Quantification of the ratio
between the longest and shortest axis of each outer (green) and inner (blue) curvature
myocardial cell in control and NC-ablated embryos. ** $p < 0.05$; *** $p < 0.001$.
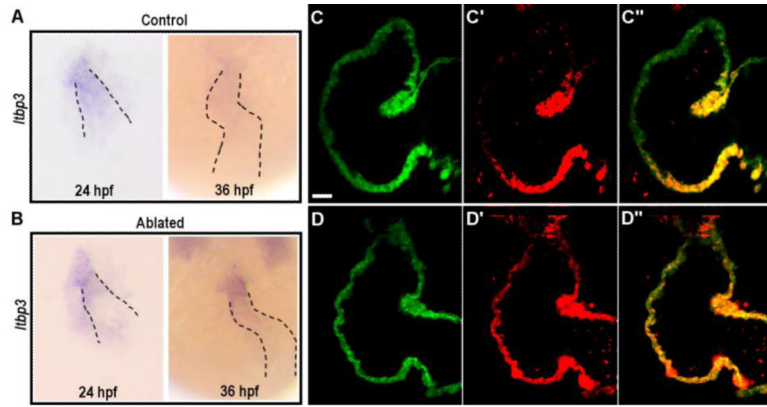
Fig. 7.
Requirement for neural crest cells in the recruitment of second heart field progenitors. (A-B) In situ hybridization for *ltbp3* in control (A) and NC-ablated embryos (B). *Ltbp3* expression is observed in both control and NC-ablated embryos at 24 hpf. By 36 hpf, *ltbp3* expression is down-regulated in control, but is persistent in NC-ablated embryos. Dashed lines indicate location of heart. (C-D'') Single z sections of ventricles from Mtz-treated *NfsB-mCherry (−); myl7:kaede* control embryo (C-C'') and Mtz-treated *NfsB-mCherry (+); myl7:kaede* NC-ablated embryos (D-D'') at 60hpf. Kaede protein photoconverted at 26 hpf are fluorescent in red whereas newly produced protein are in green. Note that ventricular cardiomyocytes at the arterial end express green Kaede whereas red Kaede proteins are present throughout the myocardium in NC-ablated embryos, indicating a defect in the recruitment of second heart field progenitors. Scale bar = 20μm.